IL-17A deficiency mitigates bleomycin-induced complement activation during lung fibrosis

Ellyse Cipolla,[*,1] Amanda J. Fisher,[†,1] Hongmei Gu,[†] Elizabeth A. Mickler,[†] Manisha Agarwal,[*] Carol A. Wilke,[*] Kevin K. Kim,[*] Bethany B. Moore,[*,‡] and Ragini Vittal[*,2]

[*]Division of Pulmonary and Critical Care Medicine and [‡]Department of Microbiology and Immunology, University of Michigan, Ann Arbor, Michigan, USA; and [†]Division of Pulmonary and Critical Care Medicine, Department of Medicine, Indiana University School of Medicine, Indianapolis, Indiana, USA

ABSTRACT: Interleukin 17A (IL-17A) and complement (C′) activation have each been implicated in the pathogenesis of idiopathic pulmonary fibrosis (IPF). We have reported that IL-17A induces epithelial injury *via* TGF-β in murine bronchiolitis obliterans; that TGF-β and the C′ cascade present signaling interactions in mediating epithelial injury; and that the blockade of C′ receptors mitigates lung fibrosis. In the present study, we investigated the role of IL-17A in regulating C′ in lung fibrosis. Microarray analyses of mRNA isolated from primary normal human small airway epithelial cells indicated that IL-17A (100 ng/ml; 24 h; $n = 5$ donor lungs) induces C′ components (C′ factor B, *C3*, and GPCR kinase isoform 5), cytokines (*IL8*, *-6*, and *-1B*), and cytokine ligands (*CXCL1*, *-2*, *-3*, *-5*, *-6*, and *-16*). IL-17A induces protein and mRNA regulation of C′ components and the synthesis of active C′ 3a (C3a) in normal primary human alveolar type II epithelial cells (AECs). Wild-type mice subjected to IL-17A neutralization and IL-17A knockout ($il17a^{-/-}$) mice were protected against bleomycin (BLEO)-induced fibrosis and collagen deposition. Further, BLEO-injured $il17a^{-/-}$ mice had diminished levels of circulating Krebs Von Den Lungen 6 (alveolar epithelial injury marker), local caspase-3/7, and local endoplasmic reticular stress-related genes. BLEO-induced local C′ activation [C3a, C5a, and terminal C′ complex (C5b-9)] was attenuated in $il17a^{-/-}$ mice, and IL-17A neutralization prevented the loss of epithelial C′ inhibitors (C′ receptor-1 related isoform Y and decay accelerating factor), and an increase in local TUNEL levels. RNAi-mediated gene silencing of *il17a* in fibrotic mice arrested the progression of lung fibrosis, attenuated cellular apoptosis (caspase-3/7) and lung deposition of collagen and C′ (C5b-9). Compared to normals, plasma from IPF patients showed significantly higher hemolytic activity. Our findings demonstrate that limiting complement activation by neutralizing IL-17A is a potential mechanism in ameliorating lung fibrosis.—Cipolla, E., Fisher, A. J., Gu, H., Mickler, E. A., Agarwal, M., Wilke, C. A., Kim, K. K., Moore, B. B., Vittal, R. IL-17A deficiency mitigates bleomycin-induced complement activation during lung fibrosis. FASEB J. 31, 5543–5556 (2017). www.fasebj.org

KEY WORDS: DAF · ER stress · C5b-9 · C3a · C5a

Interleukin 17A (IL-17A) has important roles in inflammation (1, 2), epithelial injury (3), and fibrosis (4–6), but the potential direct impact of IL-17A on complement (C′) activation and the resulting lung injury and tissue fibrosis in the pathogenesis of idiopathic pulmonary fibrosis (IPF) has not been established. It has also been reported that at optimal physiologic doses, the combination of IL-17A and C′ may even participate in the process of

ABBREVIATIONS: α-SMA, α-smooth muscle actin; Ad-IL-17R:Fc, adenovirus encoding soluble murine IL-17 receptor fusion protein; Ad-LUC, adenovirus encoding firefly luciferase; AEC, alveolar epithelial cell; *atf*, activating transcription factor; BALF, bronchoalveolar lavage fluid; BiP, ER chaperone Ig heavy-chain–binding protein; BLEO, bleomycin; C′, complement; C3a, C′ component 3a; C5b-9, terminal C′ complex; Crry, C′ receptor-1 related isoform Y; CXCL, chemokine (C-X-C motif) ligand; DAF, decay-accelerating factor; *eif2a*, eukaryotic translation initiation factor 2A; ER, endoplasmic reticulum; ERAD, ER-associated protein degradation; HRP, horseradish peroxidase; IL-17A, interleukin 17A; IPF, idiopathic pulmonary fibrosis; IRE, inositol-requiring enzyme; KL-6, Krebs Von Den Lungen 6; MUC-1, cell surface–associated mucin isoform 1; *os9*, osteosarcoma 9; *pdia3*, protein disulfide isomerase associated 3; PERK, PKR-like ER kinase; RBC, red blood cell; RNAi, RNA interference; SAEC, small airway epithelial cell; *serp1*, stress-associated endoplasmic reticulum protein 1; siRNA, small interference RNA; *vimp1*, p97/valosin-containing protein-interacting membrane protein

[1] These authors contributed equally to this work.

[2] Correspondence: Department of Medicine, Division of Pulmonary and Critical Care Medicine, University of Michigan, 4065 BSRB, Zina Pitcher Place, Ann Arbor, MI 48109, USA. E-mail: rvittal@med.umich.edu

doi: 10.1096/fj.201700289R

This article includes supplemental data. Please visit *http://www.fasebj.org* to obtain this information.

phagocytosis of microbes in the presence of vaccine-induced antibodies (7). However, repeated exposure to IL-17A has been shown to induce a positive feedback regulation of C′ in multiple cell types, including tracheal epithelium (2), human proximal tubular epithelium (8), human colonic subepithelial myofibroblasts (9), and skin fibroblasts (10). C′ activation—an essential arm of innate immunity—is initially beneficial to the clearance of microbes and damaged cells, but the local release of anaphylatoxins primes the cells to synthesize profibrotic genes that eventually lead to fibrosis. Therefore, a better understanding of the interlinked immunologic mechanisms of lung remodeling is essential to address a complex disease such as IPF.

Alveolar epithelial cells (AECs) have long been reported as victims of the surrounding inflammatory microenvironment in IPF (11), and a recent single-cell RNA sequencing report by Whitsett and colleagues (12) suggested that individual epithelial cells purified from IPF lungs frequently coexpresses selective markers for AECs (types I and II) and the conducting airways, demonstrating indeterminate states of differentiation not seen in normal lung development. Our prior reports showed compelling evidence that indicate epithelial injury related to C′ activation in primary normal human small airway epithelial cells (SAECs) (13) and IL-17A-mediated epithelial-to-mesenchymal transition in immortalized normal rat AECs (3). Therefore, in our current study, we investigated the role of IL-17A in C′ activation in normal primary human AECs and SAECs. Epithelial injury in IPF is strongly related to endoplasmic reticulum (ER) stress (14–17) and the role of IL-17A in ER stress has been reported in viral infection (18) and LPS exposure (1). Further, AECs subjected to inflammatory exposure and ER stress are reportedly susceptible to AEC permeability, apoptosis, and cell death, as indicated by levels of Krebs Von Den Lungen 6 (KL-6)/cell surface–associated mucin isoform 1 (MUC-1) (19–23), caspase-3/7 (24), and TUNEL (25). Our prior reports on epithelial injury have implicated the signaling interactions between IL-17A and TGF-β (3) and those between C′ and TGF-β (13). We have reported C′ activation in the murine bleomycin (BLEO)-induced lung fibrosis model, wherein we detected elevated local levels of the anaphylatoxins [active C′ component 3a (C3a) and C5a] and the soluble terminal C′ complex (C5b-9) (26). Other reports of C′ have shown C4d deposition in chronic lung transplant rejection (27) and prevention of sepsis- and LPS-induced lung fibrosis by blockade of C5 protein (28) (releases C5a *via* convertase) and C3 convertase (29), respectively. We used a clinically relevant murine model to mimic patients with IPF who present ongoing fibrosis (30, 31) and showed that the therapeutic blockade of receptors for C3a or C5a mitigates lung fibrosis and systemic TGF-β activity (26). Wills-Karp and colleagues (2) have shown that severe asthma is driven by dysregulated C3a/C5a control of the IL-23–T helper 17 (T_h17) axis, which leads to excessive IL-17A production. This effect occurs as a result of a shift from C5a-driven tolerance toward C3a-driven T_h17 responses at the airway surface. To date, however, the specific link between IL-17A–driven inflammation and C′ activation which eventually lead to pulmonary fibrosis has not been established.

The purpose of the current study was to investigate the role of IL-17A in the regulation of C′ activation. Toward this end, we employed the low-dose chronic injury model of lung fibrosis, and used 3 modes of intervention, which included *il17a*$^{-/-}$ mice, bioneutralization of IL-17A with adenoviral vectors that express the soluble murine receptor fusion protein, and a therapeutic intervention with small interference RNA (siRNA) specific to *il17a*. Our studies of *il17a*$^{-/-}$ mice revealed a critical role for IL-17A in mediating C′ activation in addition to cellular apoptosis, alveolar injury, and ER stress. Our IL-17A neutralization studies confirmed that loss of IL-17A bioactivity prevented the loss of epithelial C′ inhibitory proteins and cellular apoptosis. Finally, our therapeutic studies arrested the progression of lung fibrosis, in addition to mitigating cellular apoptosis and both C′ and collagen deposition. In addition, our *in vitro* observations reveal that IL-17A robustly induces C′-related gene and protein synthesis in both normal primary human airway and AECs. Collectively, these studies demonstrate that although lung remodeling is triggered by multiple mechanisms, limiting C′ activation by neutralizing IL-17A is a potential mechanism in ameliorating lung fibrosis.

MATERIALS AND METHODS

Cell culture

Normal primary human type II AECs (hAECs; Cell Biologics, Chicago, IL, USA) were grown in human alveolar epithelial basal medium supplemented with serum and growth factors (Cell Biologics). The cells were seeded at 70% confluence and incubated in 5% CO_2–95% air. Before stimulation, the cells were growth arrested in basal medium alone for 1 h. Normal primary human SAECs (Cambrex Biosciences, Walkersville, MD, USA) from 5 donor lungs were grown in small airway basal medium supplemented with growth factors (Cambrex Biosciences). Before stimulation, the cells were growth arrested for 1 h in 0.01% serum or 1:100 growth factor–containing medium.

Antibodies and other reagents

The antibodies used for immunoblot analysis or immunofluorescent labeling are as follows: decay-accelerating factor (DAF)-clone H-319 (sc-9156); and vinculin-clone7F9 (sc-73614) (Santa Cruz Biotechnology), C3a receptor (C3aR; NBP1-61567), and C5a receptor (C5aR; NBP2-15649; Novus Biologicals, Littleton, CO, USA). Recombinant proteins used in this study were human IL-17A (14-8179; BD Biosciences, Franklin Lakes, NJ, USA). All other reagents, unless otherwise specified, were from Millipore-Sigma (St. Louis, MO, USA).

Animal studies

The Animal Care and Use Committee at the University of Michigan and Indiana University School of Medicine approved the animal protocols. BLEO (0.025 U) was instilled intratracheally in C57-BL6 mice (8 wk of age; The Jackson Laboratory, Bar

Harbor, ME, USA), as previously described (26, 30, 31), with minor modifications.

Human studies

Plasma samples from patients with IPF were obtained through the National Institutes of Health, National Heart, Lung, and Blood Institute (Bethesda, MD, USA) Lung Tissue Research Consortium. Patient demographics of these samples have been reported (13) and are presented in this report (**Table 1**). All protocols were approved by the institutional review boards of the University of Michigan and Indiana University School of Medicine.

Microarray analysis

SAECs were treated with IL-17A (100 ng/ml) for 24 h. RNA was isolated, and cDNA was subjected to microarray analysis (Affymetrix; Thermo Fisher Scientific, Waltham, MA, USA) by the Microarray Core (University of Texas Southwest Medical Center, Dallas, TX, USA).

Real-time PCR

Real-time PCR was performed on cDNA from cell lysates, as reported in several publications (3, 13, 26, 30, 31), by using gene-specific Taqman assays (Thermo Fisher Scientific). The semi-quantitative real-time PCR data for each target gene was expressed as $2^{-\Delta\Delta Ct}$ relative quantitation *vs.* endogenous β-actin, with error bars representing the SE of triplicate reactions.

Western blot analysis of cell lysates

Cell lysates were subjected to immunoblot analysis, as has been described (26).

ELISA

Conditioned medium collected from replicate human *in vitro* studies was measured for active C3a by the MicroVue C3a Plus EIA Kit (Quidel Corp., San Diego, CA, USA), according to the manufacturer's instructions. Acellular bronchoalveolar lavage fluid (BALF) specimens derived from *il17a*$^{-/-}$ mice or mice treated with *il17a*-specific siRNA were used to measure the soluble form of C5b-9 with the Terminal C′ Complex C5b-9 Bioassay ELISA kit (U.S. Biologic Life Sciences, Salem, MA, USA), per the manufacturer's instructions. The active forms of C3a and C5a were measured in the BALF samples by using the mouse C′ fragment 3a and 5a ELISA kits (My Biosource, San Diego, CA, USA), respectively, per the manufacturer's instructions. Murine plasma was measured for KL-6/MUC1 with the Mouse Krebs Von Den Lungen 6 ELISA Kit (BG-MUS11425; Novateinbio, Woburn, MA, USA).

TABLE 1. *Baseline and pulmonary function characteristics of IPF patients*

Characteristic	Data, means ± SEM, $n = 23$	Range
Age (yr)	64.2 ± 1.7	48–80
Male (%)	65.2	
Smoking status (%)		
Current smoker	8.7	
Former smoker	30.4	
Never smoker	56.5	
Smoking (pack yr)[a]	34.2 ± 5.2	5–66
Pulmonary function test		
FEV1%	86.0 ± 4.8	48–138
FVC%	72.0 ± 4.3	36–108
DLCO%[a]	46.0 ± 3.5	14–94
CPI	51.9 ± 2.6	36–76

All participants were Caucasian. CPI, composite physiologic index; DLCO%, carbon monoxide diffusing capacity percentage predicted; FEV1%, forced expiratory volume in 1 s percentage predicted; FVC%, forced vital capacity percentage predicted. [a]Data missing ($n = 1$).

Immunofluorescence staining

AECs were fixed with −20°C methanol for 5 min. Cells were washed and incubated with antibodies against DAF (1:50) and the corresponding concentration of IgG, followed by incubation with the secondary antibody FITC-labeled horseradish peroxidase (HRP)-linked IgG (1:40; Jackson ImmunoResearch Laboratories, West Grove, PA, USA), for 1 h each. Nuclei were counterstained with (DAPI; Roche, Indianapolis, IN, USA). Staining was visualized by an i90 fluorescence microscope and images captured with NIS-Elements v.2.0 (both from Nikon, Melville, NY, USA).

Tissues were deparaffinized according to standard protocols and permeabilized with proteinase K (10 μg/ml in 10 mM Tris-HCl) for 30 min at 37°C. Nonspecific binding sites were blocked with bovine serum albumin (1 mg/ml) in 50 mM Tris-HCl for 10 min at 37°C. Incubation with the primary antibody ZO-1 (1:50; Zymed, Carlsbad, CA, USA) and α-SMA (1:50; Dako, Carpinteria, CA, USA) was followed by incubation with the secondary antibodies rhodamine and FITC-labeled HRP-linked IgG (1:40; Jackson ImmunoResearch Laboratories), for 1 h each. Nuclei were counterstained with DAPI. Staining was visualized by an i90 fluorescence microscope and images were captured with NIS-Elements v.2.0 (Nikon).

For the TUNEL assay, tissue sections were subjected to the same protocol as described above until the nonspecific blocking stage. TUNEL$^+$ cells were detected with *In Situ* Cell Death Detection Kit, Fluorescein (Roche). Nuclei were counterstained with DAPI. To quantitate apoptosis, at least 3 mice per group were examined, and a blinded observer counted the number of TUNEL$^+$ and DAPI$^+$ cells in 3 independent fields per mouse. At least 300 cells were analyzed per condition.

Caspase-3/7 assay

This assay detects caspase-3/7 activity based on the cleavage of a profluorescent DEVD peptide-rhodamine 110 substrate [(Z-DEVD)2-R110]. The reagent is prepared by combining equal volumes of buffer and substrate (1:1). The contents were mixed and incubated for 2 h, and the fluorescent signal was measured. The reagent permeabilizes the cells to release the caspase, delivers the profluorescent substrate, and provides optimized conditions to stabilize caspase activity. Upon cleavage of the substrates by the respective caspase, aminoluciferin is liberated and contributes to the generation of light in a luminescence reaction. The resulting luminescent signal is directly proportional to the amount of caspase activity present in the sample. In the absence of active caspase, the caspase substrates do not act as substrates for luciferase and thus produce no light.

Murine PCR microarrays

Total RNA was isolated from cells with an RNeasy Mini Kit (Qiagen, Valencia, CA, USA) and was reverse transcribed by using qScript cDNA SuperMix (Quanta BioSciences, Foster City,

CA, USA). Murine lung mRNA was used to generate cDNA. The Mouse Unfolded Protein Response RT^2 Profiler PCR Array (v.3.0; Qiagen) was used according to the manufacturer's instructions, and array data (Supplemental Data) were analyzed by using PCR Array Data Analysis software (Qiagen). The semiquantitative real-time PCR data for each target gene were expressed as $2^{-\Delta\Delta Ct}$ relative quantitation *vs.* endogenous control, with error bars representing the SEM.

Neutralization of IL-17A bioactivity

Neutralization of circulating IL-17A was performed as described (3, 5), with an adenovirus encoding soluble murine IL-17A receptor fusion protein (Ad-IL-17R:Fc), a generous gift from Dr. Jay K. Kolls (Pittsburgh, PA, USA) (32). The control vector, an adenovirus serotype 5 vector encoding the firefly gene luciferase, was purchased from Welgen (Worcester, MA, USA). Recombinant adenovirus expressing a fusion protein consisting of the murine IL-17RA extracellular domain with the murine IgG CH2 and CH3 domains was generated by subcloning the murine IL-17R cDNA (16) (*Eco*RI–**Sal*I) into pACCMV (obtained from Robert Gerard, University of Texas Southwestern Medical Center, Dallas, TX, USA), which contains (sequentially) 1.3 map units of sequence taken from the left end of the adenovirus 5 (Ad5) genome, the cytomegalovirus (CMV) early promoter; the pUC19 polylinker, simian virus 40 splice, and poly(A) signaling sequences; and map units 9 through 17 of the AdS genome. The recombinant plasmid was cotransfected into the 293 cell packaging line, together with the large adenoviral plasmid pJM17 (obtained from Frank L. Graham McMaster University, Hamilton, ON, Canada) by a calcium phosphate coprecipitation method. As described by Graham and Prevec (16), 293 cells constitutively express the adenoviral E1A and E1B proteins and support the replication of ElA-defective mutants. pJM17 supplies the remainder of the AdS genome, but its size exceeds the packaging limit for adenovirus. Adenoviral genomes formed by recombination between the pJM17 vector and the pACCMV vector containing the inhibitor expression construct were replication defective and were effectively packaged to form infectious virions. C57-BL6 mice were subjected to tail vein injections of Ad-lL-17R:Fc or an adenovirus encoding firefly luciferase (Ad-LUC) at 10^9 plaque forming units (PFU) per animal. Three days later, these mice were subjected to BLEO injury. Three weeks later, the mice were euthanized.

Immunohistochemistry

Staining for DAF and IL-17A was performed on 4 μm tissue sections, according to a published description, with slight modifications (13). For IL-17A, antigen epitopes were exposed by using Triton X-100 in PBS (0.1%; 10 min) followed by incubation with the primary antibody (1:500; R&D Systems, Minneapolis, MN, USA). Sections were then subjected to the protocol described in the manufacturers' instructions in the ABC Staining Kit (Vector Laboratories, Burlingame, CA, USA) and the Fast Red Substrate kit (HK182-5K; Biogenex, San Ramon, CA, USA). In brief, sections obtained from paraffin-embedded, formalin-fixed lungs underwent antigen retrieval treatment, followed by 5 min peroxide and protein blocks (1× Power Block; Biogenex). The sections were then incubated with the following primary Abs: rabbit anti-mouse C′ receptor-1 related isoform Y (Crry; 1:200) and rabbit anti-mouse DAF (1:200; Santa Cruz Biotechnology) and the corresponding rabbit IgG (Jackson ImmunoResearch Laboratories). The sections were washed and incubated with MACH 2 Rabbit HRP-Polymer (Biocare, Concord, CA, USA) for 30 min and then stained with ImmPACT DAB (Vector Laboratories) for 2 min. Nuclei were counterstained with hematoxylin.

In vivo delivery of RNA interference

Single-duplex siRNA sequences that targeted *il17a* or nontargeting control (ϕ) siRNA (Dharmacon Technologies, Pittsburgh, PA, USA) were used.

The siRNA sequences used in the *in vivo* experiments are: nontargeting (ϕ) siRNA: sense, 3′-CGGUAACAACGCGUACACGUU-5′, antisense, 5′-CGUGUACGCGUUGUUACCGUU-3′; *il17a* siRNA: sense, 3′-CUUUCAGGGUCGAGAAGAUUU-5′, antisense, 5′-AUCUUCUCGACCCUGAAAGUU-3′. In brief, 50 μg of siRNA suspended in 50 μl volume was instilled oropharyngeally in the mice.

Hemolytic activity

To determine the percentage of C′-mediated hemolysis, we used a published protocol with minor modifications (33). In brief, we measured triethanolamine-C′ hemolysis (TA-CH). We used sheep erythrocytes (CS1112S; Colorado Serum, Denver, CO, USA) as a positive control to determine 100% lysis in ammonia lysis buffer. The absorbance of the assay at 100% lysis was set at 0.5. Two sets of coated red blood cells (RBCs) added to diluted normal or IPF plasma (1:50) and TA-CH buffer were prepared. One set of these samples was incubated at room temperature, and the second set was incubated at 30°C for 30 min. The 96-well flat-bottomed plate was tapped every 10 min during the period of incubation. At the end of this period, TA-CH buffer was added. Reactants were centrifuged, and the supernatants were read at 540 nm.

Statistical analyses

Results are expressed as means ± SEM. A Student's *t* test and 1-way ANOVA with Bonferroni *post hoc* test were performed with Prism v.3.0 for Windows (GraphPad, San Diego, CA, USA) (26). Significance level was set at $P < 0.05$.

RESULTS

IL-17A activates C′ by modulating the mRNA and protein expression of the C′ components *in vitro*

Microarray gene analyses (Affymetrix; Thermo Fisher Scientific) of normal primary human SAECs exposed to IL-17A for 24 h revealed a ~5- and ~1.75-fold induction of *C3* and C′ factor B mRNA, respectively (**Table 2**; $N = 5$ donor lungs), and ~1.4-fold induction of *GRK5.* This positive feedback regulation by IL-17A is corroborated by findings in murine tracheal epithelium (2), skin fibroblasts (10), human proximal tubular epithelium (8), and human colonic subepithelial myofibroblasts (9). We also observed ~4.3- and 2-fold induction of *IL8* and *-6*, respectively; and a ~1.6-fold induction of *IL1B*. Further, upregulation of chemokine (C-X-C motif) ligand (*CXCL)* -1, -2, -3, -5, -6, and -16 was observed. We used RNA isolated from normal primary human AECs exposed to IL-17A for 24 h and detected the transcript induction of the C′ components *C3*, *C5*, *C′ factor B*, *C3aR1*, and *C5aR1* (**Fig. 1*A***). Immunoblot

TABLE 2. *IL-17A upregulates C′-related genes in normal human primary small airway epithelial cells*

Functional category	Affymetrix ID	Gene	Gene name	IL-17A		
				P	FDR	Fold *vs.* control
C′-related protein	17006949	*CFB*	C′ factor B	7.55E–03	3.62E–01	1.74
	16867784	*C3*	C′ component 3	3.52E–05	1.31E–01	5.17
	16709822	*GRK5*	GPCR kinase 5	2.12E–03	2.92E–01	1.40
Chemokine ligands	16967794	*CXCl1*	CXCL 1	8.81E−-03	3.70E−-01	1.85
	16976844	*CXCL2*	CXCL 2	3.92E−-04	2.05E−-01	1.94
	16976833	*CXCL3*	CXCL 3	6.27E−-04	2.29E−-01	2.75
	16976827	*CXCL5*	CXCL 5	7.25E−-05	1.52E−-01	10.97
	16967779	*CXCL6*	CXCL 6	7.59E−-03	3.62E−-01	3.22
	16840113	*CXCL16*	CXCL 16	2.20E−-02	4.63E−-01	1.59
Interleukins	16901986	*IL1B*	IL-1β	1.52E−-03	2.67E−-01	1.63
	17044177	*IL6*	IL-6 (IFN-β2)	5.42E−-04	2.28E−-01	2.08
	16967771	*IL8*	IL-8	1.89E−-04	1.75E−-01	4.34

FDR, false discovery rate.

analyses of AEC lysates revealed a loss of the C′ inhibitor DAF and an induction of C3aR and C5aR (Fig. 1*B*). Further, we corroborated our findings on *C3* mRNA induction by measuring active C3a by ELISA (Fig. 1*C*). We observed a dose-dependent increase in C3a synthesis by the AECs that was significant at the higher doses of 10 and 100 ng/ml. Finally, we confirmed our observations on IL-17A-mediated loss of DAF (Fig. 1*D*) by performing immunocytochemistry analyses to assess DAF localization. Our findings indicated the loss of membrane-bound DAF in human AECs exposed to IL-17A. Collectively, our findings indicated that IL-17A regulates the components of the C′ cascade, at both the transcription and the translational levels.

IL-17A deficiency protects against BLEO-induced lung fibrosis, collagen deposition, and lung injury

To define the role of IL-17A in a BLEO model of lung fibrosis and epithelial injury, we used *il17a*$^{-/-}$ mice. We determined the temporal expression pattern of local *il17a*

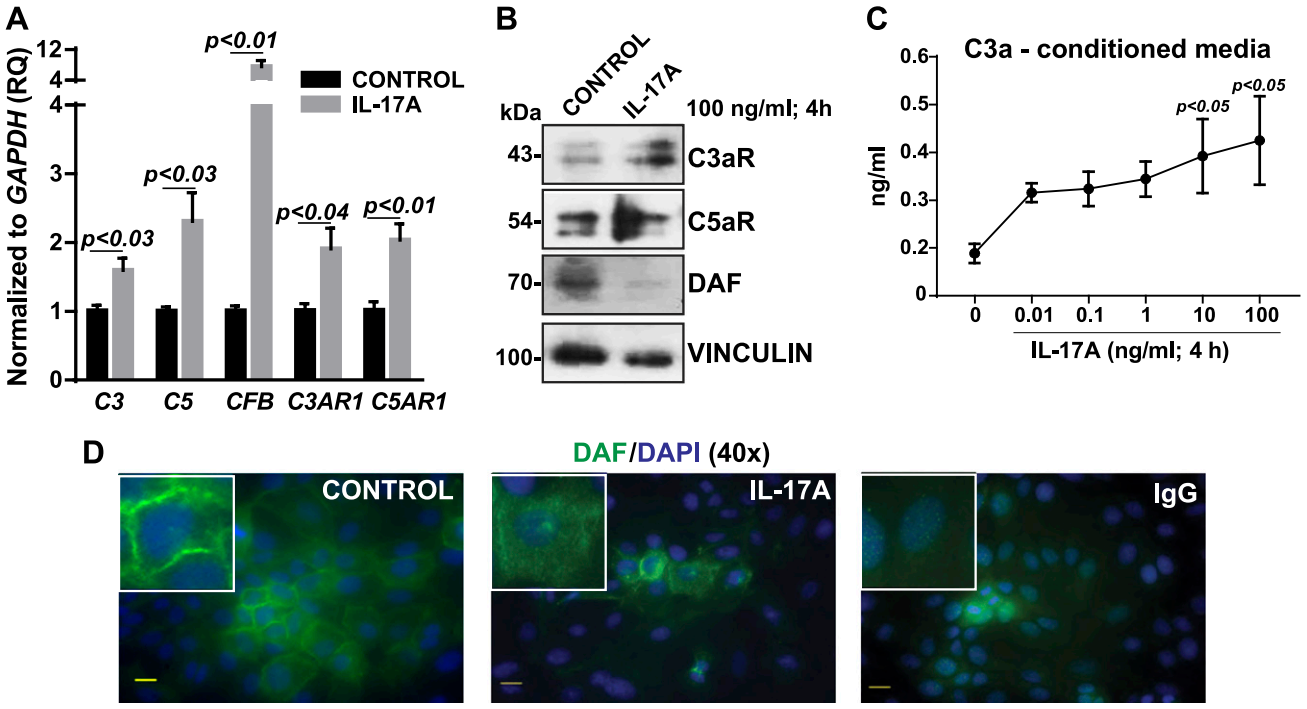

Figure 1. IL-17A activates C′ by modulating the mRNA and protein expression of the C′ components *in vitro*. *A*) Normal human primary AECs were exposed to recombinant human IL-17A (100 ng/ml; 24 h). Subsequent to RNA isolation, cDNA was generated and subjected to real-time quantitative PCR analyses. Means ± SEM; Student's *t* test. *B*) Protein lysates from AECs exposed to recombinant human IL-17A (100 ng/ml; 4 h) were subjected to immunoblot analysis against C3aR, C5aR, DAF, and vinculin. *C*) Conditioned medium collected from AECs exposed to the indicated doses of IL-17A for 4 h was analyzed for active C3a by ELISA. Means ± SEM. *D*) AECs exposed to IL-17A (100 ng/ml; 4 h) were methanol fixed, immunostained for DAF, and counterstained with DAPI. Results represent 3 independent experiments. Scale bars, 100 μm.

mRNA in BLEO-injured wild-type mice. Whole-lung mRNA analyses demonstrated that *il17a* levels in the injured lungs were increased by over ~2-fold by d 7 (**Fig. 2*A***). As shown in the schema in Fig. 2*B*, wild-type and *il17a*$^{-/-}$ mice were subjected to BLEO injury and euthanized at d 21. We then determined collagen deposition quantitatively by using the standard hydroxyproline assay on the left lung (Fig. 2*C*) and observed significantly lower levels of collagen compared to that in the diseased wild-type group. Histopathological assessments show lung architecture (hematoxylin and eosin; Fig. 2*D*) and connective tissue distribution (Masson's blue trichrome). BLEO-injured wild-type mice were severely scarred, whereas *il17a*$^{-/-}$ mice injured with BLEO had near normal lung architecture. Our results confirm those in a previous report (4) that *il17a*$^{-/-}$ mice subjected to BLEO injury are protected from lung fibrosis and collagen deposition.

We next investigated the effects of BLEO on epithelial injury in *il17a*$^{-/-}$ mice. Reports showed that circulating KL6/MUC-1 levels reflect greater alveolar permeability in sleep apnea (34), during acute exacerbations of IPF (19, 20), in patients with rapid IPF progression (21), and is a good candidate prognostic marker in IPF (22, 23). We measured KL6/MUC-1 in the plasma of wild-type and *il17a*$^{-/-}$ mice with BLEO injury and detected lower plasma KL6/MUC-1 in the *il17a*$^{-/-}$ mice (**Fig. 3*A***) suggesting a suppression of BLEO-mediated AEC injury. Further, data in Fig. 3*B* showed lower levels of caspase-3/7 in *il17a*$^{-/-}$ mice with BLEO injury compared with those in wild-type mice. Taken together, these data suggest that *il17a*$^{-/-}$ mice in this model are protected from BLEO-induced lung fibrosis and AEC injury.

Since epithelial injury in IPF is strongly related to ER stress (14–17), we addressed ER stress in our model. Prior reports indicate that IL-17A-dependent lung injury is related to ER stress during viral infection (18) and LPS exposure (1). Buildup of large amounts of misfolded protein in the ER leads to activation of the unfolded protein response (UPR) pathways, which initially protect the cells, but eventually lead to apoptosis. The UPR involves the activation of 3 transmembrane sensors—PKR-like ER kinase (PERK), ATF6, and inositol-requiring enzyme (IRE)-1—all of which are initially bound by ER chaperone Ig heavy-chain–binding protein (BiP). UPR triggers BiP to release these sensors wherein, PERK decreases protein translation *via* induction of phospho-eIF2α (eukaryotic

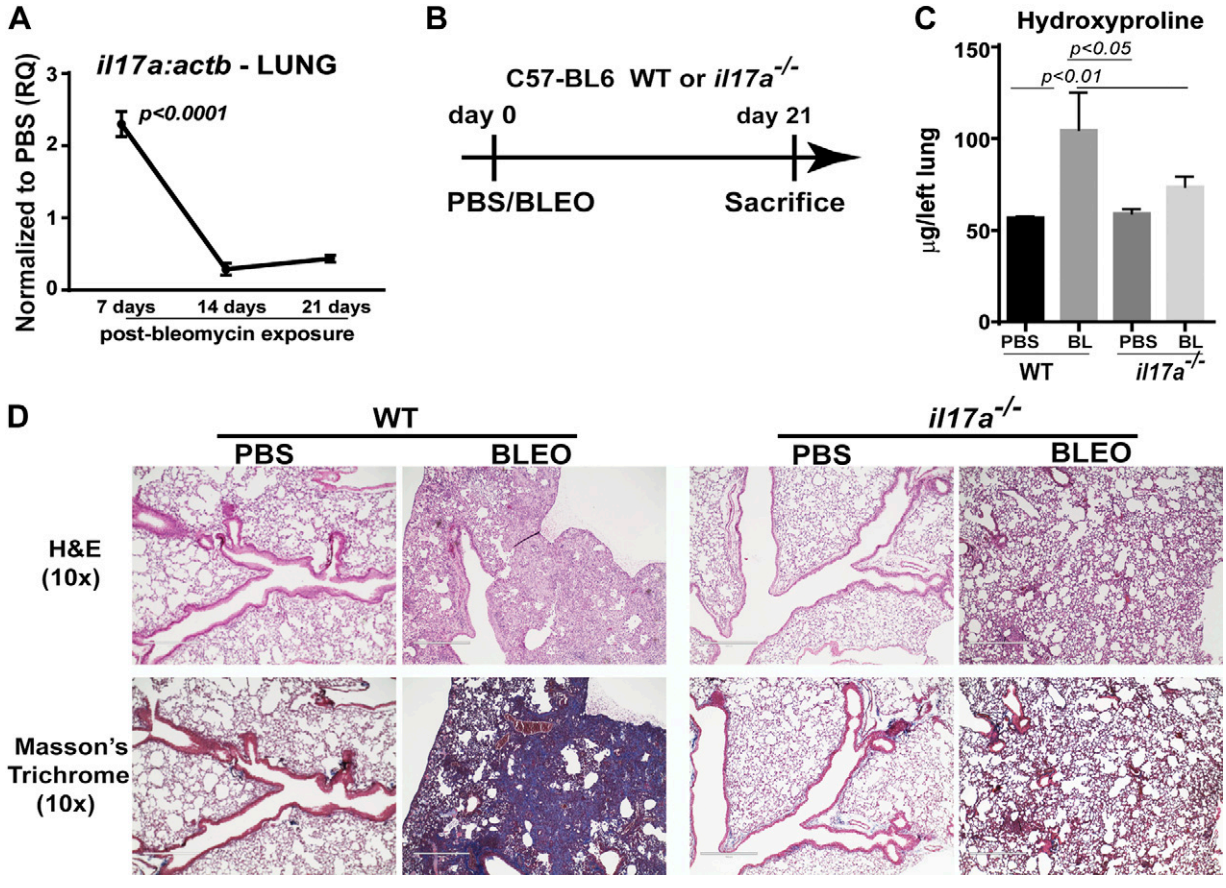

Figure 2. IL-17A deficiency protects against BLEO-induced lung fibrosis and collagen deposition. *A*) C57-BL6 wild-type mice were subjected to an intratracheal instillation of PBS or BLEO (0.025 U) on d 0 and euthanized at the indicated time points. RNA isolated from lung homogenates was subjected to real-time quantitative PCR. Means ± SEM; Student's *t* test. *B*) Time line of exposure of mice to PBS or BLEO until euthanasia. *C*) Left lungs were analyzed for hydroxyproline (n = 11–12/group). Means ± SEM; 1-way ANOVA and Bonferroni. *D*) Histopathologic examination showed that BLEO-induced fibrosis and collagen deposition were lower in the *il17a*$^{-/-}$ mice. Results are representative of 3 independent experiments. Scale bars, 100 µm.

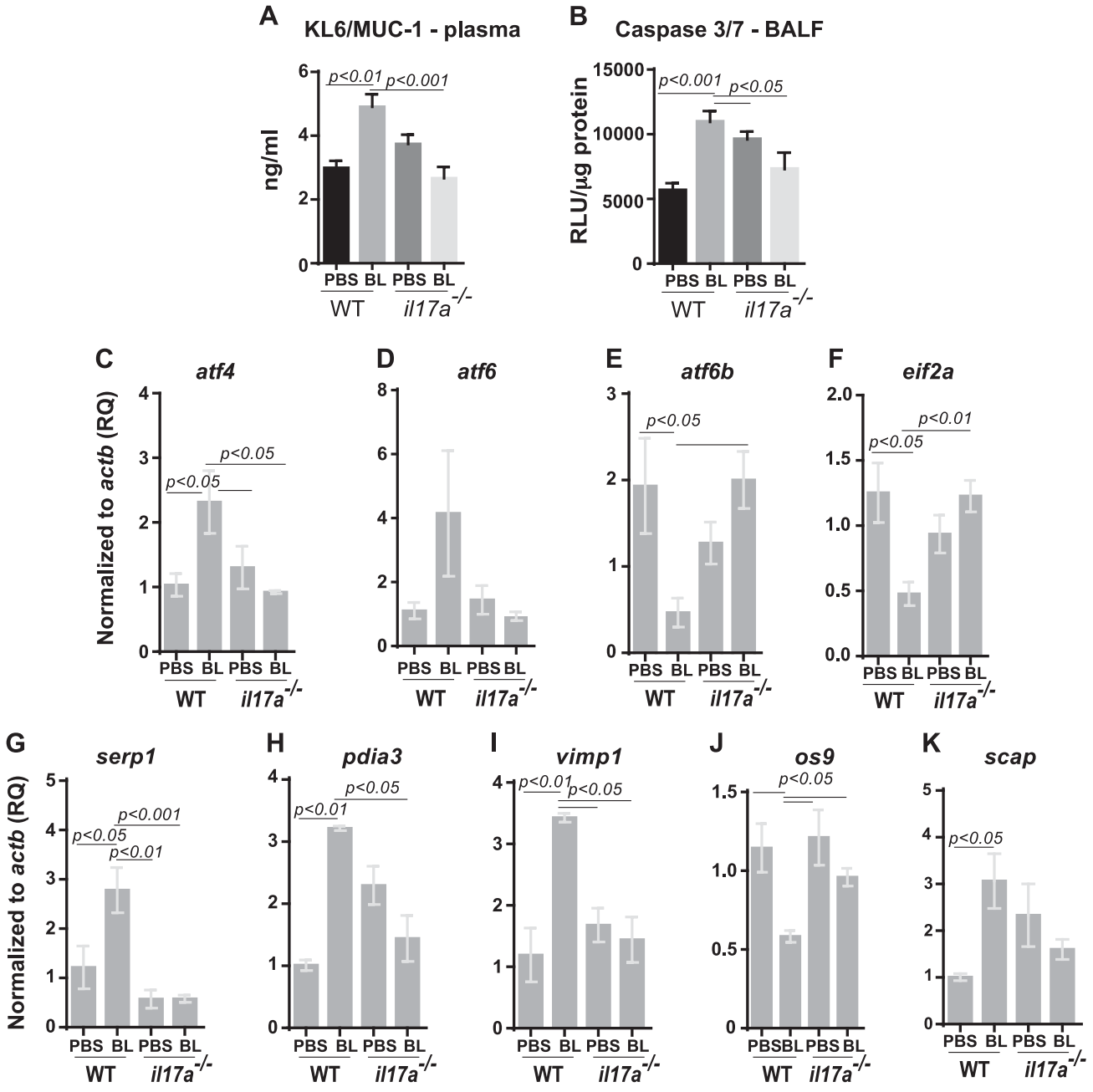

Figure 3. IL-17A deficiency protects against BLEO-induced cellular apoptosis and ER stress in the lung. *A*) Plasma from lungs described in Fig. 2*B* was analyzed for the AEC marker KL6/MUC-1 by ELISA (n = 11–12/group). Means ± SEM; 1-way ANOVA and Bonferroni. *B*) Supernatants of lung homogenates from the right lungs were subjected to caspase-3/7 luciferase assay (n = 11–12/group). Means ± SEM; 1-way ANOVA and Bonferroni. *C–K*) RNA was isolated from right lung homogenates, and cDNA was subjected to real-time PCR reactions. The specific genes were *atf4* (*C*), *atf6* (*D*), *atf6b* (*E*), *eif2a* (*F*), *serp1* (*G*), *pdia3* (*H*), *vimp1* (*I*), *os9* (*J*) and *scap* (*K*) (n = 5–6/group). Means ± SEM; 1-way ANOVA and Bonferroni (*F–I, K*), Newman-Keuls (*C, E, J*).

translation initiation factor), ATF6 induces the synthesis of folding chaperone proteins like BiP, and IRE-1 induces the synthesis of protein degradation enzymes. Notably, mRNA analyses of the lungs of BLEO-injured *il17a*$^{-/-}$ mice revealed lower levels of ER stress as indicated by lower *atf4* expression (Fig. 3C), which is activated by the PERK pathway; a lower *atf6* trend in conjunction with higher levels of *atf6* inhibitor *atf6b* (Fig. 3*D*, *E*); and more protein translation and less protein folding, as indicated by lower levels of eukaryotic translation initiation factor 2A (*eif2a*; Fig. 3*F*) and of protein disulfide isomerase family A (*pdia3*) (Fig. 3*H*), respectively. Again, *eif2a* and *pdia3* are triggered by the PERK pathway (35). We observed downregulation of stress-associated ER protein 1 (*serp1*; Fig. 3*G*; or ribosome-associated membrane protein 4) which is a co-chaperone and an interacting partner for the epithelial Na^+ channel β-subunit (βENaC). We observed downregulation of p97/valosin-containing protein-interacting membrane protein (*vimp1*) (Fig. 3*I*), which is associated with the ER-associated protein degradation (ERAD) or the IRE-1 pathway. We also observed the recovery of osteosarcoma amplified 9 (*os9*) (Fig. 3*J*; amplified

in osteo-sarcomas), which is also a component of the ERAD pathway. This gene is a specific binding partner of the Na-K-2Cl cotransporter (36). Finally, although we observed the upregulation of sterol regulatory element-binding protein, a cleavage-activating protein (Fig. 3*K*) in response to BLEO injury, we detected no changes in *il17a*$^{-/-}$ mice with BLEO injury. The above findings present several ER stress–related genes regulated by expression of IL-17A. Collectively, our observations provided compelling evidence of the role of IL-17A in lung injury in our model.

IL-17A deficiency protects against BLEO-induced local C′ activation

We next investigated the local effects of *il17a* deficiency on the C′ components active C3a and active C5a and the terminal C′ complex soluble C5b-9. Increased levels of C3a and C5a in BALF were reported in transfusion-related acute lung injury (37) and in chronic rejection after lung transplantation (38). We have reported that BLEO injury induces local C3a and C5a levels at d 14 that persist at d 28 (26). We have also reported that blocking receptors for C3a and C5a in mice with fibrotic lungs, effectively suppressed local C3a, C5a, and C5b-9 levels (26). Elevated tissue deposition of C5b-9 was reported during the acute rejection phase after lung transplantation (37). In this study, we observed that BLEO-injured mice with *il17a* deficiency have lower levels of local C3a (**Fig. 4*A***) and C5a (Fig. 4*B*), and soluble C5b-9 (Fig. 4*C*), compared to wild-type mice with BLEO injury. Collectively, these results support a role for IL-17A in driving C′ activation in the pathogenesis of lung fibrosis.

Neutralization of IL-17A prevents BLEO-induced lung fibrosis, cellular apoptosis, and the loss of C′ inhibitory proteins

To further confirm the role of IL-17A in the development of lung fibrosis and C′ activation, we used Ad-IL-17R:Fc, a vector encoding a soluble murine fusion protein that neutralizes circulating IL-17A and IL-17F by preventing the binding to their receptors and activation of downstream signaling. We have reported that neutralizing IL-17A with the use of Ad-IL-17R:Fc blocks chronic lung allograft rejection (5) and local TGF-β expression (3). Thus, in this study we hypothesized that blocking IL-17A/F from binding to their receptors would prevent BLEO-induced lung fibrosis and C′ activation. C57-BL/6 mice were administered i.v. injections of Ad-IL-17R:Fc or Ad-LUC 3 d before BLEO injury (**Fig. 5*A***). It should be noted that Kolls *et. al* (39) have demonstrated that only IL-17A can be blocked by a soluble receptor protein, whereas IL-17F requires a membrane-bound IL-17 receptor. We observed that mice which received adenoviral vectors expressing IL-17R:Fc had lower levels of lung fibrosis (Fig. 5*B*) and IL-17A expression (Fig. 5*C*). Furthermore, immunofluorescence analysis revealed high levels of the myofibroblast differentiation marker, α-smooth muscle actin (α-SMA; staining in green) expression in the fibrotic foci (Fig. 5*D*; top) of lungs in the control vector Ad-LUC group, and this effect is suppressed in the Ad-IL-17R:Fc group. Moreover, the epithelial marker, zonula occludens-1 (ZO-1-staining in red), is well defined in the lung architecture of normal mice. Furthermore, the BLEO-injured group that received Ad-IL-17R:Fc was protected from cellular injury, as indicated by TUNEL staining analyses (Fig. 5*D*; bottom). We have reported that IL-17A mediates the loss of DAF and Crry (rodent analog of the human CD46) in normal immortalized rat AECs *in vitro* (38). We have also reported the loss of DAF and Crry in murine models of obliterative bronchiolitis (38). Further, we reported the loss of DAF and CD46 in the lung epithelium of patients with IPF compared with normal lungs (13). Our previous data demonstrated that C′ activation is significantly higher in mice with lung fibrosis (26). In this report, panels in Fig. 5*E* show that normal lungs have abundant expression of the early C′ inhibitors or inhibitors of the C3 and C5 convertases DAF and Crry, on both the airway and the alveolar epithelial cells. BLEO injury in the Ad-LUC group resulted in loss of these epithelial proteins. Ad-IL-17R:Fc group protected against loss of the C′ inhibitors Crry and DAF. Taken together, our studies further confirm the role of IL-17A in regulating the C′ cascade in the pathogenesis of lung fibrosis.

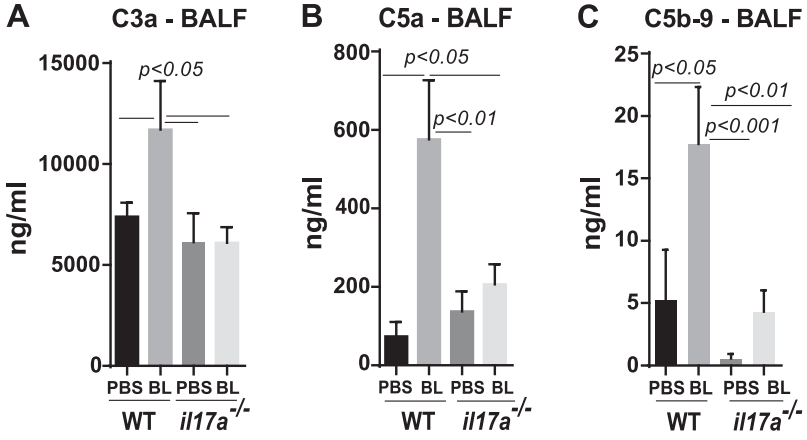

Figure 4. IL-17A deficiency protects against BLEO-induced local C′ activation. The BALF samples collected for the analysis shown in Fig. 2 were also analyzed for C3a (*A*), C5a (*B*), and C5b-9 (*C*) levels by ELISA (n = 7–8/group). Means ± SEM. One-way ANOVA, Newman-Keuls (*A*, *C*), and Bonferroni (*B*).

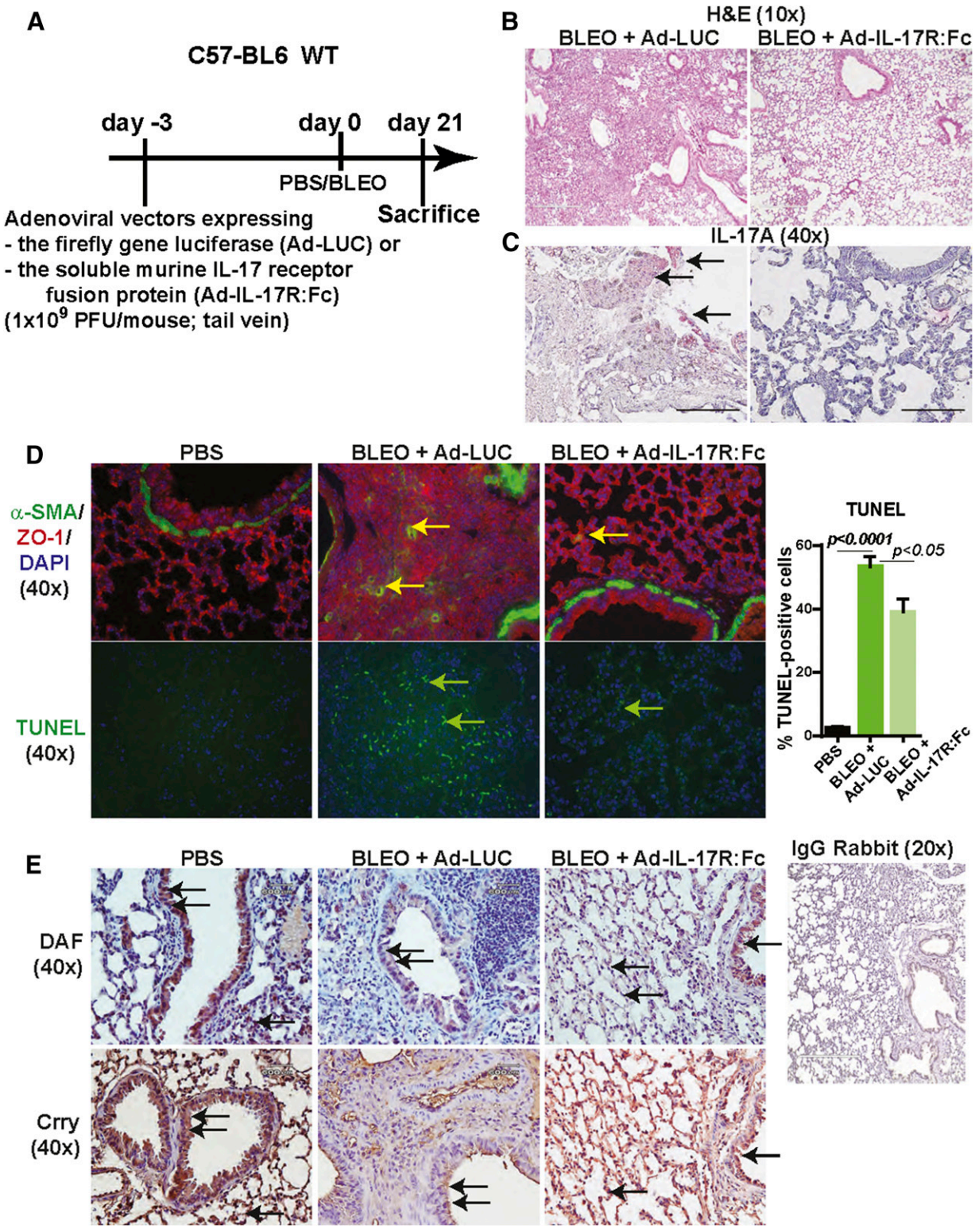

Figure 5. Neutralization of IL-17A prevents BLEO-induced lung fibrosis, apoptosis, and loss of C′ inhibitors. *A*) C57-BL6 mice received tail vein injections of the adenoviral vectors 3 d before BLEO injury and then were euthanized 21 d after injury. *B*) Histopathologic examination with hematoxylin and eosin indicates scarred lung in the Ad-LUC groups, which is prevented with administration of the Ad-IL-17R:Fc. *C*) Tissues were immunostained with antibodies against IL-17A, using secondary alkaline red phosphatase and counterstained with hematoxylin and eosin. *D*) Top: colocalization of ZO-1 and α-SMA using fluorescent labeling in the lungs of Ad-LUC and Ad-IL-17R:Fc groups. Nuclei were counterstained with DAPI. Bottom: TUNEL staining with the analyses of number of cells staining TUNEL$^+$ ($n = 5$/group). Means ± SEM; 1-way ANOVA and Bonferroni. *E*) Immunostaining of the C′ inhibitors DAF and Crry expression in the epithelial cells of lungs of Ad-LUC and Ad-IL-17R:Fc groups. Normal expression of these proteins are diminished or lost in the Ad-LUC group with BLEO injury, and this is presented in the Ad-IL-17R:Fc despite BLEO injury.

RNA interference–mediated gene silencing of *il17a* mitigates progression of fibrosis and the lung deposition of collagen and C′

We next examined the effects of the targeted suppression of *il17a* expression using the RNA interference (RNAi) approach in a clinically relevant model of lung fibrosis. We have reported this model and the extent of fibrosis (26, 30, 31). BLEO-injured mice with significantly scarred lung tissue were subjected to oropharyngeal instillation of siRNA specific to *il17a* or nontargeting control siRNA (**Fig. 6*A***). Figure 6*B* demonstrates the gene silencing efficacy of the siRNA in BLEO-injured tissues. Figure 6*C* supports our hypotheses that lack of expression of IL-17A mediates a profound antifibrotic effect, with significant suppression of collagen deposition as confirmed by measuring

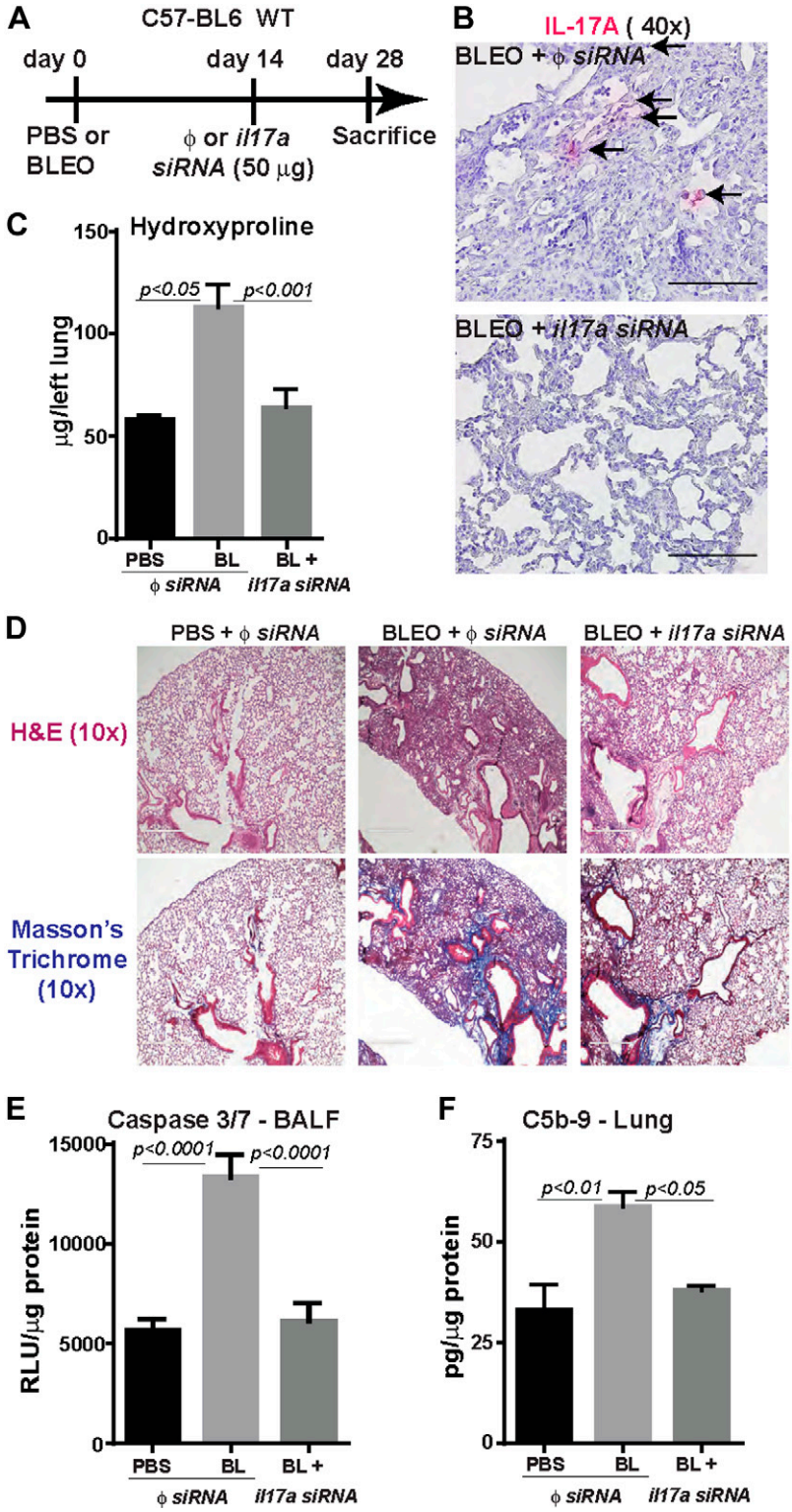

Figure 6. RNAi-mediated gene silencing of *il17a* mitigates progression of fibrosis and lung deposition of collagen and C′. *A*) PBS or BLEO (0.025 U) was instilled intratracheally in C57-BL6 mice on d 0, followed by oropharyngeal instillation of 50 μg RNAi on d 14. Tissues were harvested on d 28. *B*) Formalin-fixed paraffin-embedded tissues were immunostained with antibodies against IL-17A using secondary alkaline red phosphatase and counterstained with hematoxylin. *C*) Left lungs were analyzed for hydroxyproline (n = 11–12/group). Means ± SEM; 1-way ANOVA and Bonferroni. *D*) Histopathological examination showed that BLEO-injured fibrotic lung and collagen deposition were reduced by silencing *il17a*. Scale bars, 100 μm. *E*, *F*) We analyzed caspase-3/7 (*E*) and C5b-9 expressions (*F*) in the supernatants of the lung homogenates by the luciferase assay and ELISA, respectively (n = 10–12/group). Means ± SEM; 1-way ANOVA and Bonferroni. Results are representative of 3 independent experiments.

hydroxyproline synthesis in the left lung. Figure 6*D* shows the lung architecture of BLEO-injured mice and the corresponding extensive collagen deposition. The mice that therapeutically received *il17a*-specific siRNA showed significant recovery and corresponding lower levels of collagen deposition. We next assessed the level of lung injury in these mice by measuring the caspase-3/7 levels (Fig. 6*E*) and observed that *il17a* siRNA-treated mice had lower levels of cellular apoptosis. We then observed the suppression of lung C5b-9 deposition in BLEO-injured mice, as measured in lung homogenates (Fig. 6*F*). Collectively, these results suggest that the therapeutic blockade of *il17a* arrests fibrotic progression with suppression of local collagen and C′ deposition.

Hemolytic activity in IPF

The involvement of the C′ system in lung host defense mechanisms has been demonstrated in several lung diseases including IPF. Our earlier reports demonstrated elevated levels of active C3a and C5a (13) and the soluble terminal C′ complex C5b-9 (26) in the plasma and BALF derived from patients with IPF and normal nonsmoking healthy subjects. In this report, we investigated the functional state of the C′ components using standard hemolytic assays in the plasma samples derived from patients with IPF and normal subjects. We detected significant functional activity in plasma of patients with IPF by using antibody-coated sheep RBCs. Plasma samples from patients with IPF induced 74 ± 8% lysis of target RBCs. We detected significantly lower levels of hemolytic activity in the plasma samples of healthy normal volunteers at 32 ± 9% lysis of target RBCs, which was not different from heat-inactivated plasma samples from patients with IPF (33 ± 5%) or those of healthy normal volunteers (23 ± 6%) (**Fig. 7**). These results provide a clinical association and relevance to our findings that suppression of C′ activation is essential to mitigate further fibrotic responses (Supplemental Data).

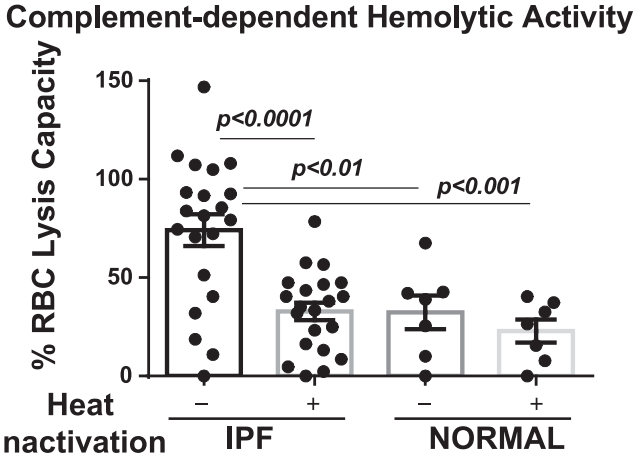

Figure 7. Hemolytic activity in IPF. Hemolytic activity was assessed in 7 normal patients and 23 with IPF, with or without heat inactivation. Means ± SEM; 1-way ANOVA and *post hoc* Bonferroni.

DISCUSSION

The present study is the first to demonstrate the role of IL-17A in driving C′ activation in a murine model of lung fibrosis. In addition to using mice that were genetically deficient in *il17a*, we employed adenoviral vectors that express soluble murine IL-17 receptor fusion protein to demonstrate that lack of IL-17A signaling suppresses local C′ activation. In addition, we show that therapeutic *RNAi*-mediated gene silencing of *il17a* mitigates lung fibrosis and local C′ and collagen deposition and adds support to the interpretation that limiting C′ by neutralizing IL-17A may be one of the potential mechanisms in ameliorating lung fibrosis. In addition to the effects of IL-17A deficiency on C′ activation, we have also confirmed that these tissues are indeed protected from cellular injury, as indicated by KL-6/MUC1, caspase-3/7, ER stress-related genes, and TUNEL analyses. Our clinical findings demonstrate evidence of C′ in patients with IPF, as indicated by the presence of hemolytic activity.

IL-17A, a major orchestrator of sustained neutrophilic mobilization (40), has been linked to IPF (4, 41). The long-prevailing hypothesis sustains the idea that AECs are victims of the surrounding inflammatory microenvironment (11). Wilson *et al.* (4) have shown that BLEO-injured lungs have high levels of IL-17A. Early reports by Strunk *et al.* (42) showed that human AECs synthesize C′ proteins, including C2, C3, C4, C5, and factor B, as detected by immunoblot techniques in AECs and whole lungs. Our microarray studies in SAECs showed that IL-17A induced mRNA expression of *IL6*, *-8*, and *-1B* in lung epithelial cells. It is possible that these cytokines enhance the local synthesis of C′ proteins and add to the milieu. Van Kooten *et al.* (8) demonstrated the role of IL-17A in regulating local inflammatory responses by showing that after a 72 h exposure to IL-17A, human proximal tubular epithelial cells synthesized C3 protein but not C2, C4, or factor H. Our current findings show that IL-17A induces the mRNA synthesis of C3, C5, and factor B as early as in 24 h in AECs (the relevant cell type in lung fibrosis) and the synthesis of active C3a as well as the protein expression of receptors for C3a and C5a within 4 h. Sugihara *et al.* (9) reported that blockade of ERK and p38MAPK prevented IL-17A-induced C3 mRNA expression by human colonic subepithelial myofibroblasts as early as 12 h. We have observed that IL-17A mediates epithelial injury *via* TGF-β-p38MAPK signaling (3) and that TGF-β, C3a, and C5a each mediate epithelial injury *via* p38MAPK activation (13). Our studies and reports by others demonstrate that local synthesis of C′ proteins is a steady source of inflammatory responses in the lung, specifically for the AECs.

The importance of IL-17A in IPF was underscored when Wilson *et al.* (4) identified elevated expression of IL-17A in BALF from a lung with regions of marked inflammatory foci within the parenchyma, surrounded by dense collagen deposits. They also reported that IL-17A-driven fibrosis is suppressed by IL-10, that IL-17A and TGF-β may have cooperative roles in the development of fibrosis, and that IL-1β-induced fibrosis, which mimics BLEO-induced fibrosis, is dependent on IL-17A (4). Other

studies also show an increasing role for T cells in murine models of IPF (43–45) and IL-17A derived from T cells associated with antigen-induced murine pulmonary fibrosis (46). Bone marrow transplantation from *il17a*$^{-/-}$ donors or treatment with anti-IL-17A neutralization antibodies at late stages attenuated pneumonitis and fibrosis in virus–infected mice who have received bone marrow transplantation, suggesting that hematopoietic-derived IL-17A is essential for development of pathology (6). Our *in vivo* studies of *il17a*$^{-/-}$ mice and a low-dose (0.025 U) model of BLEO studied over a period of 3 wk show that, indeed, chronic injury is prevented by *il17a* deficiency. This model allows us to study the mechanisms of lung fibrosis in the context of C′ activation in a remodeled lung and the effects of therapeutic administration of *il17a* siRNA. Further, we showed that *il17a* mRNA expression is significantly high compared to that in a normal lung and drops to baseline at d 14. It is likely that the protein expression would be sustained until d 14. Our model contrasts with the report by Wilson *et al.* (4), in that they used triple instillations of a high dose (0.15 U) of BLEO and terminated their studies in 1 wk. They also reported significant weight loss in the BLEO-injured mice, despite *il17a* deficiency at 1 wk. We found significant local and systemic lung injury at d 21, as indicated by caspase-3/7 and the AEC injury marker KL6/MUC-1.

IL-17A has been reported to induce ER stress and exacerbate LPS-induced lung injury (1) and respiratory syncytial virus-induced lung pathology (18). Elevated local levels of BLEO-induced IL-17A and IL-6 levels were exacerbated by increased extracellular adenosine levels and progressive lung fibrosis (47). Korfei *et al.* (15) reported that severe ER stress response in the AECs of patients with sporadic IPF may underlie the apoptosis of this cell type and development of fibrosis in IPF, by observing high levels of ATF4 and -6 in AECs. Yuan *et al.* (48) have reported that inhibition of the ER stress pathway protects against cigarette smoke extract–induced human bronchial epithelial cell apoptosis by regulating the activity of eIF2α. Pacello *et al.* (49) reported that PDIA3 promotes the proinflammatory response elicited by cells in response to infections. SERP1 is a novel cochaperone and regulator of epithelial Na(+) channel expression (50). SERP1 controls the early biogenesis of membrane proteins (50). Hofmann *et al.* (52) reported that fine mapping and mRNA expression studies pointed to OS9 as the most likely candidate for the underlying risk factor for sarcoidosis. The OS9 protein plays an important role in ERAD and acts during TLR-induced activation of myeloid cells (51). We have observed upregulation of *atf4*, *serp1*, *pdia3*, *vimp1*, and *os9*, with downregulation of *atf6b* and *eif2a*, as expected. Both *vimp1* and *os9* belong to the ERAD pathway, but *vimp1* is indeed downregulated in *il17a*$^{-/-}$ mice with BLEO injury, the trend is reversed in the case of *os9.* It should be noted that because the murine model in our studies addressed fibrosis rather than the inflammatory phase. Our studies present compelling evidence for IL-17A-mediated local ER stress in chronic lung fibrosis, as indicated by the regulation of the related genes.

It has been reported that IL-17RA (the receptor for IL-17A) expression was necessary in both hematopoietic and parenchymal cells to enable significant glomerular C3 deposition in experimental glomerulonephritis (52). House dust mite–mediated local C3a synthesis was mitigated using IL-17A monoclonal antibodies in experimental allergic asthma (2). As we have previously identified that blockade of receptors to C3a and C5a mitigates progression of lung fibrosis (26), we explored the possibility that C′ activation may underlie IL-17A-mediated lung fibrosis. In the current report, we demonstrate a previously unexplored role and a direct link for IL-17A in the regulation of C′ activation and progression of lung fibrosis. Notably, in our studies, the direct association between IL-17A and C′ activation held up across a wide spectrum of IL-17A interventions. We used 3 approaches to demonstrate the role of IL-17A in regulating C′ in the pathogenesis of lung fibrosis. We used *il17a*$^{-/-}$ mice to demonstrate the role of IL-17A in driving local C′ activation. We also used the prophylactic approach *via* adenoviral vectors overexpressing soluble murine IL-17A receptor fusion protein to bioneutralize IL-17A before BLEO injury and showed protection against lung fibrosis and loss of C′ inhibitors. Lastly, and most importantly, we used the therapeutic approach of *il17a*-specific siRNA-mediated gene silencing and demonstrated protection against lung fibrosis and mitigated local deposition of both collagen and C′. To our knowledge, this is the first report to demonstrate the therapeutic efficacy of IL-17A inhibition in arresting the progression of lung fibrosis. We have bolstered our findings by presenting data on caspase-3/7 in the same tissues that were tested for C′ deposition. Thus, our studies support our claim that neutralizing IL-17A will ameliorate fibrosis by limiting C′ activation.

Finally, our clinical results demonstrate the presence of C′ as measured by hemolytic activity. Lambré *et al.* (54) reported the presence of C′ in IPF BALF samples and measured the hemolytic activity. C′ activation leads to the release of numerous C′ components that are potent modulators of macrophage, monocyte, and lymphocyte functions such as phagocytosis, release of lysosomal enzymes, oxygen metabolite generation, and antibody synthesis (53). Our results show the systemic levels of C′ activity in IPF patients. Clearly, C′ activity is significantly higher in patients with IPF than in normal healthy volunteers. When these plasma samples from IPF patients were heat inactivated, then the activity dropped 50-fold to a level compared to that of normal volunteers. Although we attempted to correlate the lung function indices with hemolytic activity, we did not detect a significant correlation owing to the wide range of activity and the low number of patients with IPF analyzed (data not shown).

Our studies present evidence, for the first time to our knowledge, which definitively links IL-17A to C′ activation and leads to the pathogenesis of fibrosis. The possible missing links in our studies would be the lack of use of more clinical samples to analyze the hemolytic activity and compare those levels with the lung function indices and with the local activity. Another possible missing link would be to substantiate our therapeutic findings by providing add-back therapy findings. Further, the combined synergistic effects of IL-17A and the anaphylatoxins

C3a and C5a, on AECs are unknown. Our studies in the current report provide compelling evidence, but our aforementioned concerns will be addressed in future studies.

CONCLUSIONS

Our studies provide a missing link between IL-17A-driven inflammation and eventual fibrosis. Although IL-17A drives ER stress and apoptosis in the lungs on one hand, it simultaneously drives the C′ cascade and augments the epithelial injury and profibrotic signaling pathways. Thus, limiting the C′ cascade by neutralizing IL-17A may be one of the potential mechanisms in ameliorating lung fibrosis. FJ

ACKNOWLEDGMENTS

This work was supported by U.S. National Institutes of Health (NIH) National Heart, Lung, and Blood Institute (NHLBI) Grants R01-HL119682 (to B.B.M.) and R01-HL109288 (to R.V.). The authors declare no conflict of interest.

AUTHOR CONTRIBUTIONS

R. Vittal conducted conception and design; E. Cipolla, A. J. Fisher, H. Gu, E. A. Mickler, M. Agarwal, and C. A. Wilke conducted the experiments and data acquisition; K. K. Kim, B. B. Moore, and R. Vittal conducted data interpretation and analyses; and R. Vittal drafted the manuscript for important intellectual content.

REFERENCES

1. Kim, S. R., Kim, H. J., Kim, D. I., Lee, K. B., Park, H. J., Jeong, J. S., Cho, S. H., and Lee, Y. C. (2015) Blockade of interplay between IL-17A and endoplasmic reticulum stress attenuates LPS-induced lung injury. *Theranostics* **5**, 1343–1362
2. Lajoie, S., Lewkowich, I. P., Suzuki, Y., Clark, J. R., Sproles, A. A., Dienger, K., Budelsky, A. L., and Wills-Karp, M. (2010) Complement-mediated regulation of the IL-17A axis is a central genetic determinant of the severity of experimental allergic asthma. *Nat. Immunol.* **11**, 928–935
3. Vittal, R., Fan, L., Greenspan, D. S., Mickler, E. A., Gopalakrishnan, B., Gu, H., Benson, H. L., Zhang, C., Burlingham, W., Cummings, O. W., and Wilkes, D. S. (2013) IL-17 induces type V collagen overexpression and EMT via TGF-β-dependent pathways in obliterative bronchiolitis. *Am. J. Physiol. Lung Cell. Mol. Physiol.* **304**, L401–L414
4. Wilson, M. S., Madala, S. K., Ramalingam, T. R., Gochuico, B. R., Rosas, I. O., Cheever, A. W., and Wynn, T. A. (2010) Bleomycin and IL-1beta-mediated pulmonary fibrosis is IL-17A dependent. *J. Exp. Med.* **207**, 535–552
5. Fan, L., Benson, H. L., Vittal, R., Mickler, E. A., Presson, R., Fisher, A. J., Cummings, O. W., Heidler, K. M., Keller, M. R., Burlingham, W. J., and Wilkes, D. S. (2011) Neutralizing IL-17 prevents obliterative bronchiolitis in murine orthotopic lung transplantation. *Am. J. Transplant.* **11**, 911–922
6. Zhou, X., Loomis-King, H., Gurczynski, S. J., Wilke, C. A., Konopka, K. E., Ptaschinski, C., Coomes, S. M., Iwakura, Y., van Dyk, L. F., Lukacs, N. W., and Moore, B. B. (2016) Bone marrow transplantation alters lung antigen-presenting cells to promote TH17 response and the development of pneumonitis and fibrosis following gammaherpesvirus infection. *Mucosal Immunol.* **9**, 610–620
7. Campos, I. B., Herd, M., Moffitt, K. L., Lu, Y. J., Darrieux, M., Malley, R., Leite, L. C., and Gonçalves, V. M. (2017) IL-17A and complement contribute to killing of pneumococci following immunization with a pneumococcal whole cell vaccine. *Vaccine* **35**, 1306–1315
8. Van Kooten, C., Boonstra, J. G., Paape, M. E., Fossiez, F., Banchereau, J., Lebecque, S., Bruijn, J. A., De Fijter, J. W., Van Es, L. A., and Daha, M. R. (1998) Interleukin-17 activates human renal epithelial cells in vitro and is expressed during renal allograft rejection. *J. Am. Soc. Nephrol.* **9**, 1526–1534
9. Sugihara, T., Kobori, A., Imaeda, H., Tsujikawa, T., Amagase, K., Takeuchi, K., Fujiyama, Y., and Andoh, A. (2010) The increased mucosal mRNA expressions of complement C3 and interleukin-17 in inflammatory bowel disease. *Clin. Exp. Immunol.* **160**, 386–393
10. Katz, Y., Nadiv, O., Rapoport, M. J., and Loos, M. (2000) IL-17 regulates gene expression and protein synthesis of the complement system, C3 and factor B, in skin fibroblasts. *Clin. Exp. Immunol.* **120**, 22–29
11. Selman, M., and Pardo, A. (2006) Role of epithelial cells in idiopathic pulmonary fibrosis: from innocent targets to serial killers. *Proc. Am. Thorac. Soc.* **3**, 364–372
12. Xu, Y., Mizuno, T., Sridharan, A., Du, Y., Guo, M., Tang, J., Wikenheiser-Brokamp, K. A., Perl, A. T., Funari, V. A., Gokey, J. J., Stripp, B. R., and Whitsett, J. A. (2016) Single-cell RNA sequencing identifies diverse roles of epithelial cells in idiopathic pulmonary fibrosis. *JCI Insight* **1**, e90558
13. Gu, H., Mickler, E. A., Cummings, O. W., Sandusky, G. E., Weber, D. J., Gracon, A., Woodruff, T., Wilkes, D. S., and Vittal, R. (2014) Crosstalk between TGF-β1 and complement activation augments epithelial injury in pulmonary fibrosis. *FASEB J.* **28**, 4223–4234
14. Lawson, W. E., Crossno, P. F., Polosukhin, V. V., Roldan, J., Cheng, D. S., Lane, K. B., Blackwell, T. R., Xu, C., Markin, C., Ware, L. B., Miller, G. G., Loyd, J. E., and Blackwell, T. S. (2008) Endoplasmic reticulum stress in alveolar epithelial cells is prominent in IPF: association with altered surfactant protein processing and herpesvirus infection. *Am. J. Physiol. Lung Cell. Mol. Physiol.* **294**, L1119–L1126
15. Korfei, M., Ruppert, C., Mahavadi, P., Henneke, I., Markart, P., Koch, M., Lang, G., Fink, L., Bohle, R. M., Seeger, W., Weaver, T. E., and Guenther, A. (2008) Epithelial endoplasmic reticulum stress and apoptosis in sporadic idiopathic pulmonary fibrosis. *Am. J. Respir. Crit. Care Med.* **178**, 838–846
16. Tanjore, H., Blackwell, T. S., and Lawson, W. E. (2012) Emerging evidence for endoplasmic reticulum stress in the pathogenesis of idiopathic pulmonary fibrosis. *Am. J. Physiol. Lung Cell. Mol. Physiol.* **302**, L721–L729
17. Ge, L., Habiel, D. M., Hansbro, P. M., Kim, R. Y., Gharib, S. A., Edelman, J. D., Königshoff, M., Parimon, T., Brauer, R., Huang, Y., Allen, J., Jiang, D., Kurkciyan, A. A., Mizuno, T., Stripp, B. R., Noble, P. W., Hogaboam, C. M., and Chen, P. (2016) miR-323a-3p regulates lung fibrosis by targeting multiple profibrotic pathways. *JCI Insight* **1**, e90301
18. Reed, M., Morris, S. H., Owczarczyk, A. B., and Lukacs, N. W. (2015) Deficiency of autophagy protein Map1-LC3b mediates IL-17-dependent lung pathology during respiratory viral infection via ER stress-associated IL-1. *Mucosal Immunol.* **8**, 1118–1130
19. Ohshimo, S., Ishikawa, N., Horimasu, Y., Hattori, N., Hirohashi, N., Tanigawa, K., Kohno, N., Bonella, F., Guzman, J., and Costabel, U. (2014) Baseline KL-6 predicts increased risk for acute exacerbation of idiopathic pulmonary fibrosis. *Respir. Med.* **108**, 1031–1039
20. Collard, H. R., Calfee, C. S., Wolters, P. J., Song, J. W., Hong, S. B., Brady, S., Ishizaka, A., Jones, K. D., King, T. E., Jr., Matthay, M. A., and Kim, D. S. (2010) Plasma biomarker profiles in acute exacerbation of idiopathic pulmonary fibrosis. *Am. J. Physiol. Lung Cell. Mol. Physiol.* **299**, L3–L7
21. Yokoyama, A., Kondo, K., Nakajima, M., Matsushima, T., Takahashi, T., Nishimura, M., Bando, M., Sugiyama, Y., Totani, Y., Ishizaki, T., Ichiyasu, H., Suga, M., Hamada, H., and Kohno, N. (2006) Prognostic value of circulating KL-6 in idiopathic pulmonary fibrosis. *Respirology* **11**, 164–168
22. Yokoyama, A., Kohno, N., Hamada, H., Sakatani, M., Ueda, E., Kondo, K., Hirasawa, Y., and Hiwada, K. (1998) Circulating KL-6 predicts the outcome of rapidly progressive idiopathic pulmonary fibrosis. *Am. J. Respir. Crit. Care Med.* **158**, 1680–1684
23. Zhang, Y., and Kaminski, N. (2012) Biomarkers in idiopathic pulmonary fibrosis. *Curr. Opin. Pulm. Med.* **18**, 441–446
24. Wheaton, A. K., Agarwal, M., Jia, S., and Kim, K. K. (2017) Lung epithelial cell focal adhesion kinase signaling inhibits lung injury and fibrosis. *Am. J. Physiol. Lung Cell. Mol. Physiol.* **312**, L722–L730
25. Choi, J. E., Lee, S. S., Sunde, D. A., Huizar, I., Haugk, K. L., Thannickal, V. J., Vittal, R., Plymate, S. R., and Schnapp, L. M. (2009) Insulin-like growth factor-I receptor blockade improves outcome in mouse model of lung injury. *Am. J. Respir. Crit. Care Med.* **179**, 212–219

26. Gu, H., Fisher, A. J., Mickler, E. A., Duerson III, F., Cummings, O. W., Peters-Golden, M., Twigg III, H. L., Woodruff, T. M., Wilkes, D. S., and Vittal, R. (2016) Contribution of the anaphylatoxin receptors, C3aR and C5aR, to the pathogenesis of pulmonary fibrosis. *FASEB J.* **30**, 2336–2350
27. Witt, C. A., Gaut, J. P., Yusen, R. D., Byers, D. E., Iuppa, J. A., Bennett Bain, K., Alexander Patterson, G., Mohanakumar, T., Trulock, E. P., and Hachem, R. R. (2013) Acute antibody-mediated rejection after lung transplantation. *J. Heart Lung Transplant.* **32**, 1034–1040
28. Addis-Lieser, E., Köhl, J., and Chiaramonte, M. G. (2005) Opposing regulatory roles of complement factor 5 in the development of bleomycin-induced pulmonary fibrosis. *J. Immunol.* **175**, 1894–1902
29. Silasi-Mansat, R., Zhu, H., Georgescu, C., Popescu, N., Keshari, R. S., Peer, G., Lupu, C., Taylor, F. B., Pereira, H. A., Kinasewitz, G., Lambris, J. D., and Lupu, F. (2015) Complement inhibition decreases early fibrogenic events in the lung of septic baboons. *J. Cell. Mol. Med.* **19**, 2549–2563
30. Vittal, R., Fisher, A., Gu, H., Mickler, E. A., Panitch, A., Lander, C., Cummings, O. W., Sandusky, G. E., and Wilkes, D. S. (2013) Peptide-mediated inhibition of mitogen-activated protein kinase-activated protein kinase-2 ameliorates bleomycin-induced pulmonary fibrosis. *Am. J. Respir. Cell Mol. Biol.* **49**, 47–57
31. Vittal, R., Mickler, E. A., Fisher, A. J., Zhang, C., Rothhaar, K., Gu, H., Brown, K. M., Emtiazdjoo, A., Lott, J. M., Frye, S. B., Smith, G. N., Sandusky, G. E., Cummings, O. W., and Wilkes, D. S. (2013) Type V collagen induced tolerance suppresses collagen deposition, TGF-β and associated transcripts in pulmonary fibrosis. *PLoS One* **8**, e76451
32. Zhang, Z., Zheng, M., Bindas, J., Schwarzenberger, P., and Kolls, J. K. (2006) Critical role of IL-17 receptor signaling in acute TNBS-induced colitis. *Inflamm. Bowel Dis.* **12**, 382–388
33. Inglis, J. E., Radziwon, K. A., and Maniero, G. D. (2008) The serum complement system: a simplified laboratory exercise to measure the activity of an important component of the immune system. *Adv. Physiol. Educ.* **32**, 317–321
34. Lederer, D. J., Jelic, S., Basner, R. C., Ishizaka, A., and Bhattacharya, J. (2009) Circulating KL-6, a biomarker of lung injury, in obstructive sleep apnoea. *Eur. Respir. J.* **33**, 793–796
35. Tavernier, S. J., Osorio, F., Vandersarren, L., Vetters, J., Vanlangenakker, N., Van Isterdael, G., Vergote, K., De Rycke, R., Parthoens, E., van de Laar, L., Iwawaki, T., Del Valle, J. R., Hu, C. A., Lambrecht, B. N., and Janssens, S. (2017) Regulated IRE1-dependent mRNA decay sets the threshold for dendritic cell survival. *Nat. Cell Biol.* **19**, 698–710
36. Seaayfan, E., Defontaine, N., Demaretz, S., Zaarour, N., and Laghmani, K. (2016) OS9 protein interacts with Na-K-2Cl co-transporter (NKCC2) and targets its immature form for the endoplasmic reticulum-associated degradation pathway. *J. Biol. Chem.* **291**, 4487–4502
37. Jiang, X., Nguyen, T. T., Tian, W., Sung, Y. K., Yuan, K., Qian, J., Rajadas, J., Sallenave, J. M., Nickel, N. P., de Jesus Perez, V., Rabinovitch, M., and Nicolls, M. R. (2015) Cyclosporine does not prevent microvascular loss in transplantation but can synergize with a neutrophil elastase inhibitor, elafin, to maintain graft perfusion during acute rejection. *Am. J. Transplant.* **15**, 1768–1781
38. Suzuki, H., Lasbury, M. E., Fan, L., Vittal, R., Mickler, E. A., Benson, H. L., Shilling, R., Wu, Q., Weber, D. J., Wagner, S. R., Lasaro, M., Devore, D., Wang, Y., Sandusky, G. E., Lipking, K., Pandya, P., Reynolds, J., Love, R., Wozniak, T., Gu, H., Brown, K. M., and Wilkes, D. S. (2013) Role of complement activation in obliterative bronchiolitis post-lung transplantation. *J. Immunol.* **191**, 4431–4439
39. McAllister, F., Henry, A., Kreindler, J. L., Dubin, P. J., Ulrich, L., Steele, C., Finder, J. D., Pilewski, J. M., Carreno, B. M., Goldman, S. J., Pirhonen, J., and Kolls, J. K. (2005) Role of IL-17A, IL-17F, and the IL-17 receptor in regulating growth-related oncogene-alpha and granulocyte colony-stimulating factor in bronchial epithelium: implications for airway inflammation in cystic fibrosis. *J. Immunol.* **175**, 404–412
40. Dong, C. (2008) Regulation and pro-inflammatory function of interleukin-17 family cytokines. *Immunol. Rev.* **226**, 80–86
41. Braun, R. K., Martin, A., Shah, S., Iwashima, M., Medina, M., Byrne, K., Sethupathi, P., Wigfield, C. H., Brand, D. D., and Love, R. B. (2010) Inhibition of bleomycin-induced pulmonary fibrosis through pre-treatment with collagen type V. *J. Heart Lung Transplant.* **29**, 873–880
42. Strunk, R. C., Eidlen, D. M., and Mason, R. J. (1988) Pulmonary alveolar type II epithelial cells synthesize and secrete proteins of the classical and alternative complement pathways. *J. Clin. Invest.* **81**, 1419–1426
43. Parra, E. R., Boufelli, G., Bertanha, F., Samorano, Lde. P., Aguiar, A. C., Jr., Costa, F. M., Capelozzi, V. L., and Barbas-Filho, J. V. (2008) Temporal evolution of epithelial, vascular and interstitial lung injury in an experimental model of idiopathic pulmonary fibrosis induced by butyl-hydroxytoluene. *Int. J. Exp. Pathol.* **89**, 350–357
44. Luzina, I. G., Todd, N. W., Iacono, A. T., and Atamas, S. P. (2008) Roles of T lymphocytes in pulmonary fibrosis. *J. Leukoc. Biol.* **83**, 237–244
45. Hackett, T. L., Warner, S. M., Stefanowicz, D., Shaheen, F., Pechkovsky, D. V., Murray, L. A., Argentieri, R., Kicic, A., Stick, S. M., Bai, T. R., and Knight, D. A. (2009) Induction of epithelial-mesenchymal transition in primary airway epithelial cells from patients with asthma by transforming growth factor-beta1. *Am. J. Respir. Crit. Care Med.* **180**, 122–133
46. Simonian, P. L., Roark, C. L., Wehrmann, F., Lanham, A. K., Diaz del Valle, F., Born, W. K., O'Brien, R. L., and Fontenot, A. P. (2009) Th17-polarized immune response in a murine model of hypersensitivity pneumonitis and lung fibrosis. *J. Immunol.* **182**, 657–665
47. Luo, F., Le, N. B., Mills, T., Chen, N. Y., Karmouty-Quintana, H., Molina, J. G., Davies, J., Philip, K., Volcik, K. A., Liu, H., Xia, Y., Eltzschig, H. K., and Blackburn, M. R. (2016) Extracellular adenosine levels are associated with the progression and exacerbation of pulmonary fibrosis. *FASEB J.* **30**, 874–883
48. Yuan, T., Luo, B. L., Wei, T. H., Zhang, L., He, B. M., and Niu, R. C. (2012) Salubrinal protects against cigarette smoke extract-induced HBEpC apoptosis likely via regulating the activity of PERK-eIF2α signaling pathway. *Arch. Med. Res.* **43**, 522–529
49. Pacello, F., D'Orazio, M., and Battistoni, A. (2016) An ERp57-mediated disulphide exchange promotes the interaction between Burkholderia cenocepacia and epithelial respiratory cells. *Sci. Rep.* **6**, 21140
50. Faria, D., Lentze, N., Almaça, J., Luz, S., Alessio, L., Tian, Y., Martins, J. P., Cruz, P., Schreiber, R., Rezwan, M., Farinha, C. M., Auerbach, D., Amaral, M. D., and Kunzelmann, K. (2012) Regulation of ENaC biogenesis by the stress response protein SERP1. *Pflugers Arch.* **463**, 819–827
51. Hofmann, S., Fischer, A., Nothnagel, M., Jacobs, G., Schmid, B., Wittig, M., Franke, A., Gaede, K. I., Schürmann, M., Petrek, M., Mrazek, F., Pabst, S., Grohé, C., Grunewald, J., Ronninger, M., Eklund, A., Rosenstiel, P., Höhne, K., Zissel, G., Müller-Quernheim, J., and Schreiber, S. (2013) Genome-wide association analysis reveals 12q13.3-q14.1 as new risk locus for sarcoidosis. *Eur. Respir. J.* **41**, 888–900
52. Ghali, J. R., O'Sullivan, K. M., Eggenhuizen, P. J., Holdsworth, S. R., and Kitching, A. R. (2017) Interleukin-17RA promotes humoral responses and glomerular injury in experimental rapidly progressive glomerulonephritis. *Nephron* **135**, 207–223
53. Lambré, C. R., le Maho, S., di Bella, G., de Cremoux, H., Atassi, K., and Bignon, J. (1986) Bronchoalveolar lavage fluid and serum complement activity in pulmonary sarcoidosis. *Am. Rev. Respir. Dis.* **134**, 238–242

Received for publication April 5, 2017.
Accepted for publication August 7, 2017.